Alexandria Engineering Journal (2023) 62, 113–127

HOSTED BY

Alexandria University

Alexandria Engineering Journal

www.elsevier.com/locate/aej
www.sciencedirect.com

Mode division multiplexing free space optics system with 3D hybrid modulation under dust and fog

Mehtab Singh [a], Sahil Nazir Pottoo [b], Moustafa H. Aly [c], Štěpán Hubálovský [d], Amit Grover [e], Debashis Adhikari [f], Preecha Yupapin [g,h,*]

[a] Department of Electronics and Communication Engineering, University Institute of Engineering, Chandigarh University, Mohali, Punjab, India
[b] Department of Electrical Engineering, UiT The Arctic University of Norway, Narvik, Norway
[c] Electronics and Communication Engineering Department, College of Engineering and Technology, Arab Academy for Science, Technology and Maritime Transport, Alexandria P.O.B. 1029, Egypt
[d] Department of Applied Cybernetics, Faculty of Science, University of Hradec Králové, Czech Republic
[e] Department of Electronics and Communication Engineering, Shaheed Bhagat Singh State University, Ferozepur, India
[f] School of EEE, VIT Bhopal University, Sehore, India
[g] Computational Optics Research Group, Science and Technology Advanced Institute, Van Lang University, Ho Chi Minh City, Viet Nam
[h] Faculty of Technology, Van Lang University, Ho Chi Minh City, Viet Nam

Received 3 January 2022; revised 13 April 2022; accepted 4 July 2022
Available online 29 July 2022

KEYWORDS

Free space optics;
3D digital modulation;
Spatial diversity;
Disaster management;
B5G/6G

Abstract Mode division multiplexing (MDM) is an emerging information transmission technique in which multiple data signals can be transmitted simultaneously on different modes of a single wavelength laser beam over a free-space channel. MDM is a potential technique for the realization of high-speed spectral efficient communication links for future generations of wireless networks. We present a novel MDM-based free-space optics (FSO) system. The system integrates a 3D hybrid modulation scheme produced by combining carrier suppressed-non-return-to-zero (CSNRZ), differential quadrature phase-shift keying (DQPSK), and polarization shift keying (PolSK) modulation schemes for beyond 100 Gbps applications. Three unrelated 40 Gbps data signals are modulated and transmitted on one optical carrier utilizing three distinct signal properties: amplitude (CSNRZ), phase (DQPSK), and polarization state (PolSK). The proposed 3D modulation scheme offers a high-capacity system, where each channel transmits 4 Gbps as compared to 1 Gbps in the case of OOK modulation. MDM using distinct Hermite Gaussian modes: (HG00 and HG01) of a laser beam is incorporated to boost the spectral efficiency and information rates of the FSO link. The proposed 120 Gbps single-channel MDM-FSO link performance is examined under the impact of different levels of dust and fog environmental conditions using quality factors and

* Corresponding author at: Computational Optics Research Group, Science and Technology Advanced Institute, Van Lang University, Ho Chi Minh City, Viet Nam.
E-mail addresses: mehtab91singh@gmail.com (M. Singh), sahil.n.pottoo@uit.no (S. Nazir Pottoo), mosaly@aast.edu, drmosaly@gmail.com (M. H. Aly), stepan.hubalovsky@uhk.cz (Š. Hubálovský), amitgrover321@gmail.com (A. Grover), debashis@vitbhopal.ac.in (D. Adhikari), preecha.yupapin@vlu.edu.vn (P. Yupapin).

Peer review under responsibility of Faculty of Engineering, Alexandria University.

https://doi.org/10.1016/j.aej.2022.07.012

received eye diagrams as the performance metrics. This system achieved optimal performances up to 1250 m (very light dust), 540 m (light dust), 170 m (moderate dust), 750 m (low fog), and 425 m (medium fog). In the worst-case scenario, the system manages to work up to a 67 m range in dense dust with a maximum attenuation of 297.38 dB/km and a 200 m distance in heavy fog with only 90 dB/km attenuation which is less than 1/3rd of the attenuation measured for dense dust event. In addition, our results and the case studies confirm that dust introduces greater signal attenuation than fog. Therefore, an encounter with a dust environment should be considered as the bottleneck issue for FSO links. The creative contribution of this paper is to put forward a bandwidth-efficient MDM-FSO-enabled B5G system that could be deployed in harsh and challenging locations at reduced visibility. This is expected to be further technically sustainable owing to the use of advanced 3D hybrid optical orthogonal modulation and therefore find use in implementing 5G and 6G cellular and data networks.

1. Introduction

As conventional modulation formats are limited to below 40 Gbps, it is of utmost importance to propose a modulation technique to enhance the capacity per channel. Recently, various modulation techniques have been discussed to augment the capacity of single-channel wireless systems [1–4]. But, the hybrid multi-dimensional modulation technique shows better results as it not only increases the speed of the channel but also increases the number of users [1]. Using hybrid modulation for more than one user can transmit data into a single channel using different parameters of a common signal. Several new modulation schemes, for instance: amplitude shift keying (ASK), frequency-shift keying (FSK), differential phase-shift keying (DPSK), and combined signaling like ASK-DPSK and DPSK-dark return-to-zero (DPSK-DRZ) have invited ample interest because of high spectral efficiency and channel capacity [2–4]. It is necessary to adopt these modulation schemes to commercialize multi-bit-per-symbol ultra-low latency optical transceiver systems. Polarization shift keying (PolSK) is considered a strong candidate in impending optical networks that provides constant energy per bit and aids to remove cross-talk amongst unicast data and multicast data signals [5,6].

The orthogonality principle in advanced modulation schemes makes it possible to transmit several kinds of data in a single channel which upturns the number of consumers and broadens the channel capacity [7,8]. The authors in [9] investigated the ASK/DPSK scheme with direct detection receivers. In [10], an orthogonal modulation type with a tunable duty cycle and extinction ratio in the optical domain is recommended, but, the effect of different atmospheric conditions like dust and fog is not considered, which is vital for next-generation FSO systems. Multi-state per symbol orthogonal modulations are expected to reach higher spectral efficiencies, ease dispersion issues, and upgrade polarization-mode dispersion (PMD) forbearance [11,12]. Many other research groups have shown interest and proposed new modulation schemes to support future GHz/THz applications [13–16].

New antenna system designs are crucial to transmit and receive wireless RF and optical signals in the GHz/THz spectrums. In [17], it is shown that by integrating slots, interdigital capacitors, spiral- and meander lines-shaped stubs, and via-holes into the antenna designs, high performances can be achieved at high broadband frequencies. In [18], innovative on-chip antennas employing metamaterials, metasurfaces, and substrate integrated waveguides to improve the frequency bandwidth and radiation properties are discussed. These techniques can enhance the effective aperture of on-chip antennas, suppress surface waves, and reduce substrate losses. Ref [19] examines various decoupling methods based on metamaterial/metasurface techniques for applications which have a direct impact on the development of the next generation wireless communication systems, such as 5G, 6G, and massive MIMO. Ref [20–22] demonstrate metamaterial-based effective techniques for automatic tuning of the antenna impedance for integration in broadband wireless communication systems.

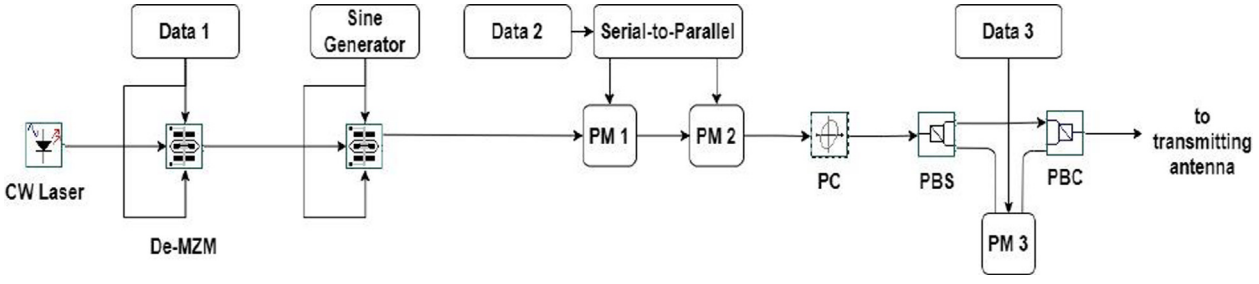

Fig. 1 Design of the transmitter station.

Table 1 Design parameters with values [1,11].

Parameter	Value
Operating frequency	193.1 THz
Input power	10 dBm
Laser linewidth	0.1 MHz
Sine frequency	40 GHz with – 90° phase
Bit rate	40 Gbps/channel
Transmitter aperture diameter	5 cm
Receiver aperture diameter	20 cm
Beam divergence angle	1.5 mrad
PIN responsivity	1 A/W
Sequence length	16,384
Sample per bit	4

Compared with conventional tuning techniques these algorithms converge rapidly close to the optimum impedance for maximum power transfer. In [23–24], a dual band operation technique using a metasurface that can control the polarization of scattered EM-waves is proposed while [25] presents RF energy harvesting circuit of high efficiency. These dual band circular polarized antennas aide in the selection of antenna geometries, for instance, the necessary dimensions, bandwidth, gain, and useful materials for the incorporation and realization in future communication systems. An automatic quantum genetic algorithm (AQGA) for automated adaptive antenna impedance tuning is proposed in [26]. The results for the AQGA tuning method cover applications across 1.4 to 5 GHz (satellite services, LTE networks, radar systems, and WiFi bands).

Towards deploying FSO-enabled B5G cellular/data network in challenging environments, in this work, an advanced hybrid optical orthogonal modulation scheme by combining CSNRZ, DQPSK, and PolSK is proposed in Section II. This reduces the bandwidth requirements of the optoelectronic devices in transceiver architecture. It has increased the capacity of the proposed system four times and achieved 4-bit/symbol orthogonal transmission without employing accurate extinction ratio amendments. A 120 Gbps MDM-FSO communication system performance is discussed under light to severe dust and fog conditions in Section III, including overwhelming results, comparison, and case studies. Section IV outlines the conclusions.

2. Implementation

Fig. 1 displays the hardware assembly of the transmitter side of the MDM-FSO system. The proposed system has been designed and evaluated using commercial OptiSystem software from Optiwave Inc. Essentially the optical transmitter consists of the components responsible for binary data generation, laser beam production, modulation, and transmitting antenna optics assembly. A 40 Gbps binary data (D_1) and a laser beam of 10 dBm tuned at 193.1 THz frequency are modulated by a

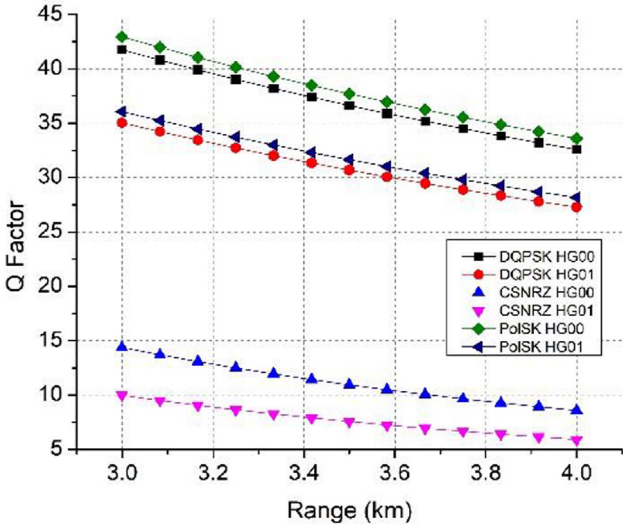

Fig. 3 Q-factor v/s range under clear climate.

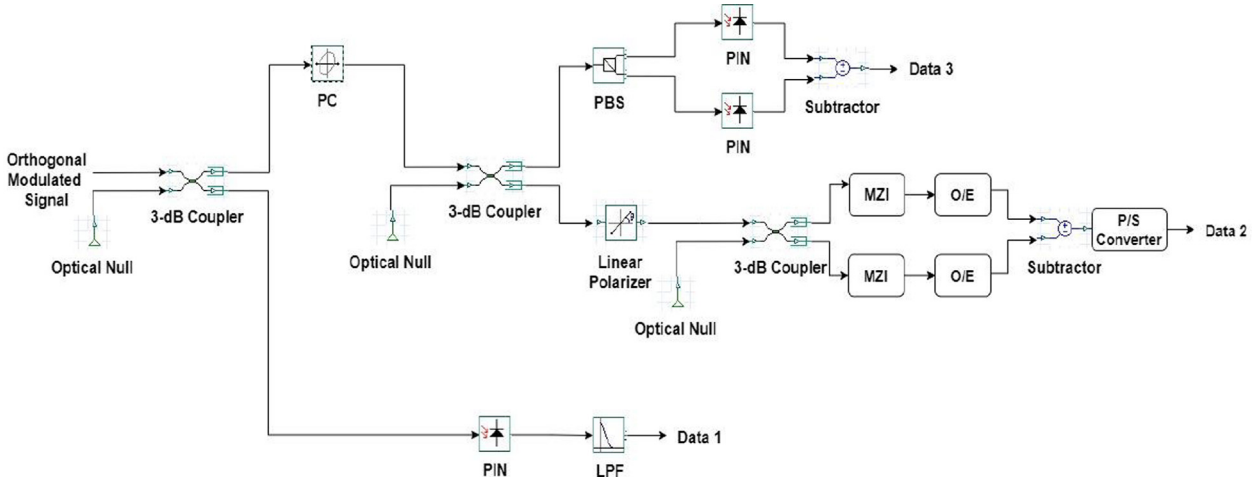

Fig. 2 Design of the receiver station.

dual-electrode Mach-Zehnder modulator (DE-MZM). This modulated signal passes through the second MZM powered by a sine generator to produce the CSNRZ signal. Another 40 Gbps binary data (D_2) is split into two analogous streams of data that drive the first and second phase modulators (PM_1/PM_2), respectively. The PM_1 phase modulates the laser beam to 0 or π. PM_2 adds a 0 or $\pi/2$ shift in phase to yield a DQPSK signal. A polarization controller (PC) directs this signal at a 45° phase angle at the input port of a polarization beam splitter (PBS). A third phase modulator (PM_3) located between parallel ends of PBS and polarization beam combiner (PBC), with their vertical ends connected, modulates the 40 Gbps binary data (D_3) in the form of PolSK signal. At this point, a 3D hybrid CSNRZ-DQPSK-PolSK data-bearing optical signal is produced and transmitted by a transmitting antenna into free space. The various design and simulation considerations undertaken in the proposed work are listed in Table 1. Numerous dust and fog weather scenarios have been

Table 2 Eye diagrams under clear climate at 4 km FSO link.

	HG00 Channel	HG01 Channel
CSNRZ	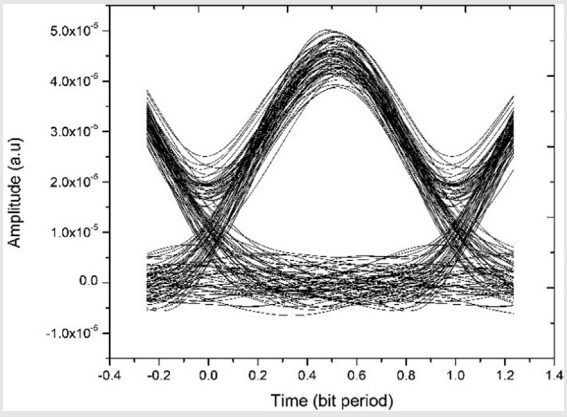	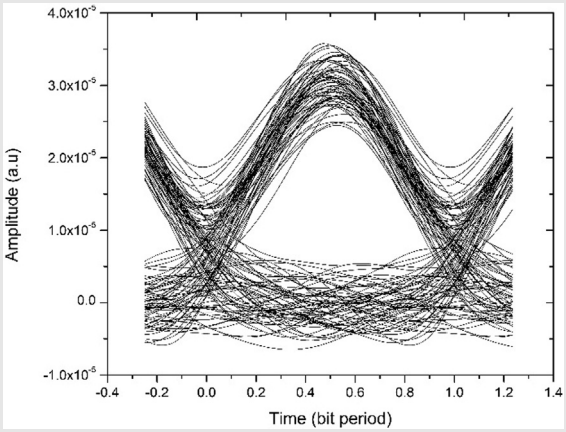
DQPSK (for in-phase signal)	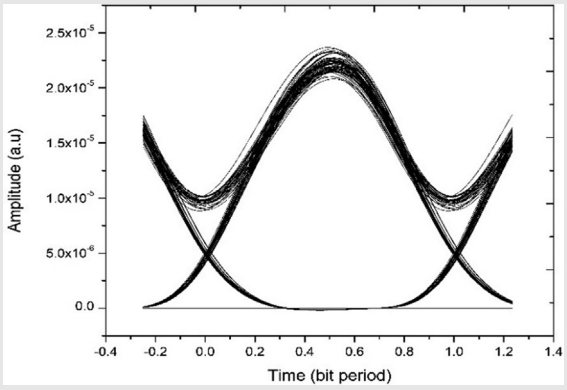	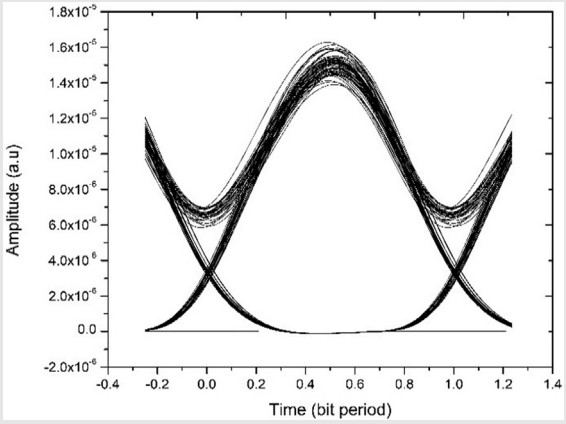
PolSK	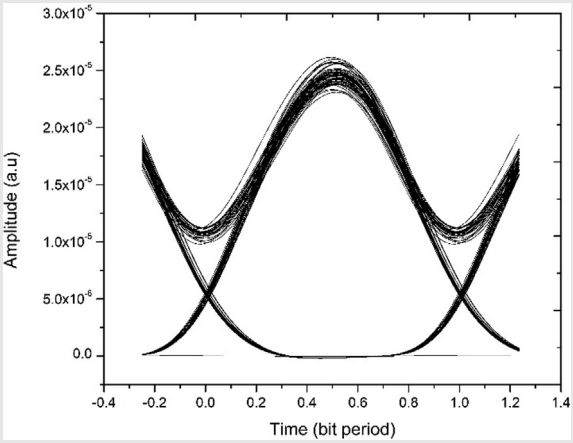	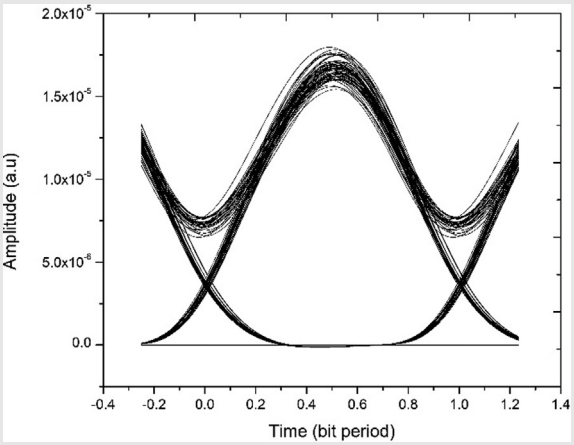

generated by varying the attenuation levels and channel losses using optical attenuator and FSO channel component factors as per the channel models.

The receiver section shown in Fig. 2 involves three discrete trails to recover the modulated orthogonal signal containing CSNRZ-DQPSK-PolSK signals. A front-end 3-dB coupler delivers a part of the detected power to the lower receiver arm consisting of a PIN photodiode and a low pass filter (LPF) for CSNRZ signal detection. Even though DQPSK and PolSK signals are also present in the detected signal, this receiver arm retrieves data encoded on intensity fluctuations only, i.e., D_1. A linear polarizer is used to detect the DQPSK signal with the ability to hold up the PolSK modulated signal. Two Mach-Zehnder interferometers and a balanced detector recover the binary data D_2. Therefore, for data retrieval from the CSNRZ signal, a 3-dB coupler, a PIN photodiode, and an LPF are required. DQPSK signal detection utilizes three 3-dB couplers, a linear polarizer, two MZIs, two optical/electrical converters, a subtractor and a parallel-to-serial converter. While two 3-dB couplers, a PBS, two PIN photodiodes, and a subtractor demodulate the PolSK signal i.e., D_3. The recovered data is fed into a lab computer for further data processing and visualization.

3. Results and discussion

This segment presents the results obtained after extensive numerical simulations for the MDM-FSO system with the 3D hybrid optical modulation scheme followed by dust/fog comparison and case studies.

3.1. MDM-FSO system in sunny weather

Fig. 3 reports the variation in quality factor (Q-factor) with the link distance for CSNRZ, DQPSK, and PolSK modulations through both HG00 and HG01 channels under a clear climate. It is evident that with increasing FSO range, the Q-factor deteriorates which confines the coverage range to 4 km. Table 2 illustrates the eye diagrams for clear weather at a 4 km distance.

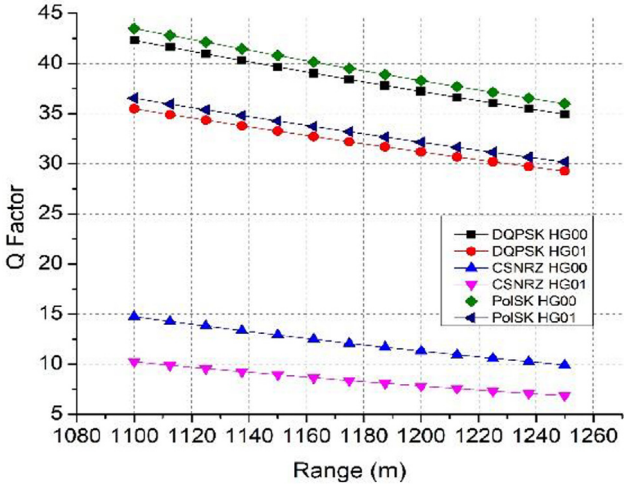

Fig. 4 Q-factor v/s range under very light dust condition.

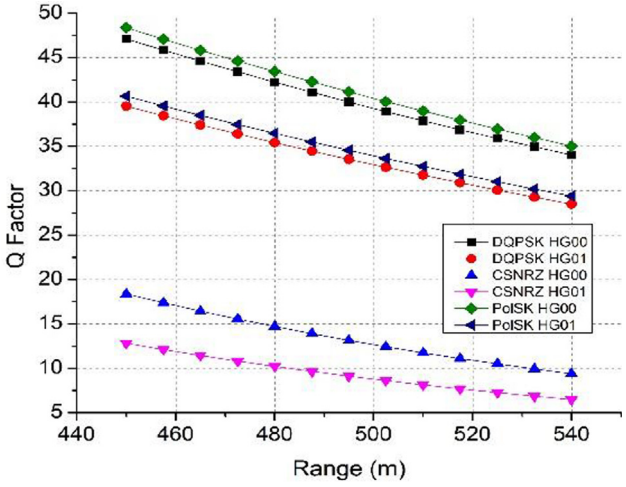

Fig. 5 Q-factor v/s range under light dust condition.

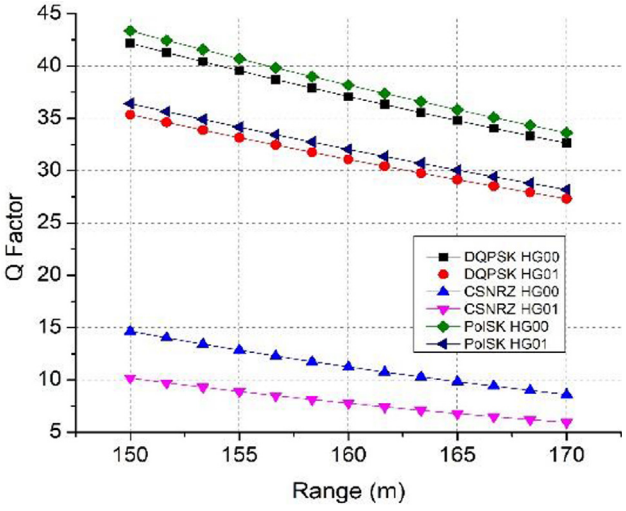

Fig. 6 Q-factor v/s range under moderate dust condition.

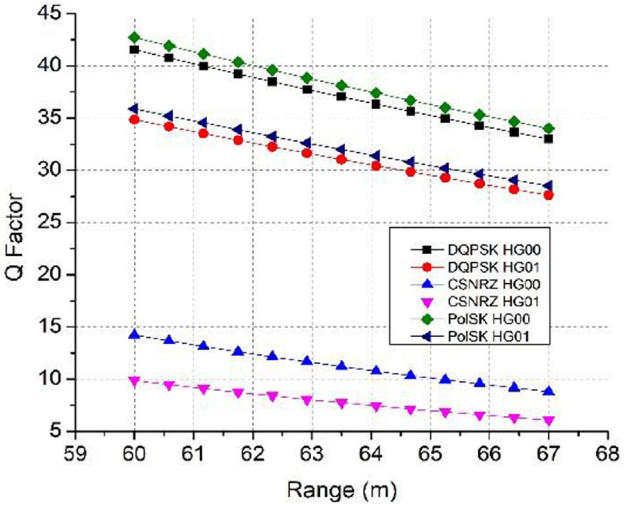

Fig. 7 Q-factor v/s range under dense dust condition.

Table 3 Received signal eye diagram at 1250 m range under very light dust condition.

	HG00 Channel	HG01 Channel
CSNRZ	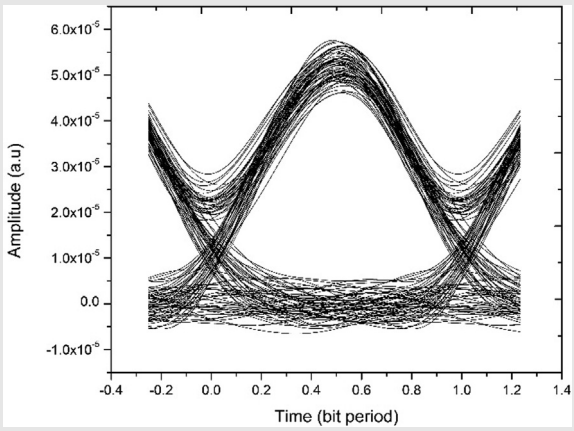	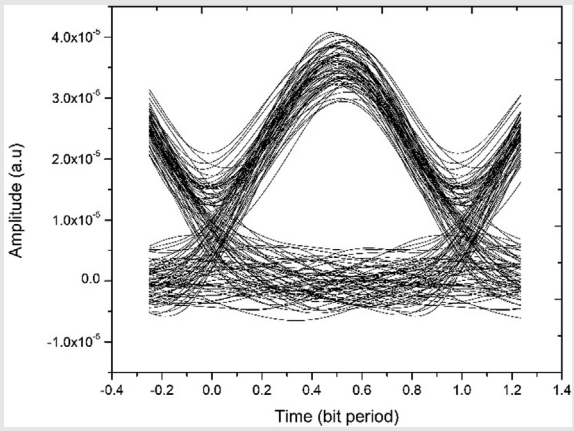
DQPSK (for in-phase signal)	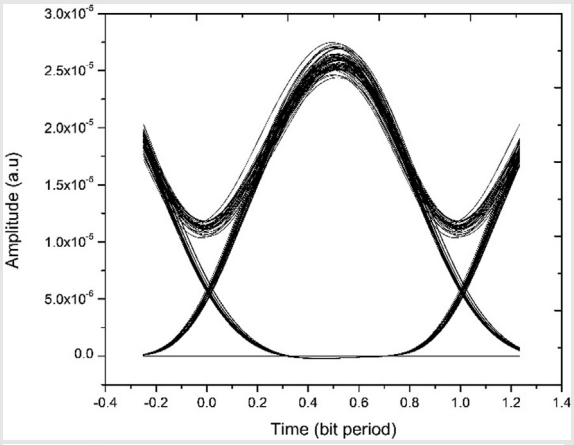	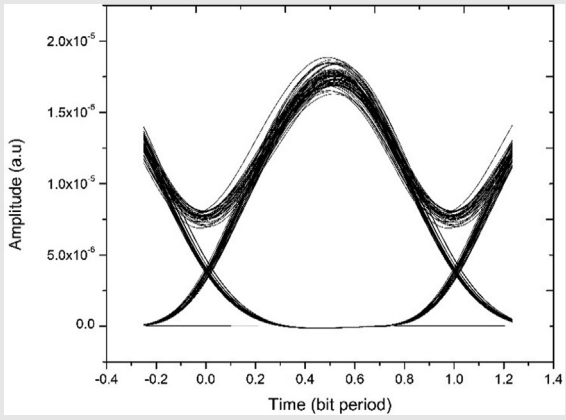
PolSK	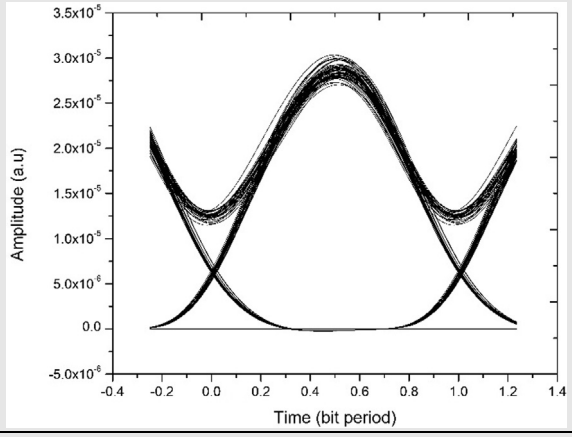	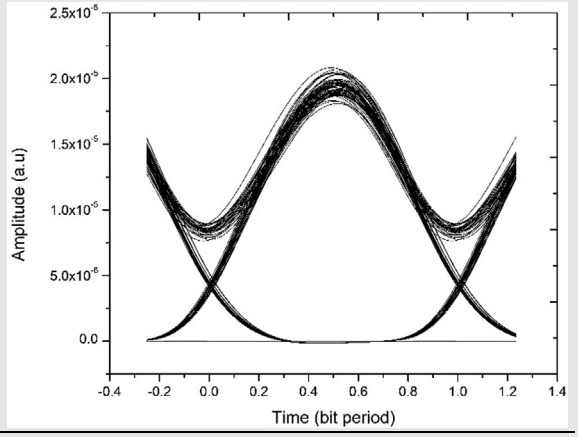

3.2. MDM-FSO system in the dust storm

Figs. 4-7 display the Q-factor of the proposed system under very light, light, moderate, and dense dust situations, respectively. It is worthwhile to emphasize that for equal reach, both DQPSK and PolSK outdistance the CSNRZ modulation since information is carried over the amplitude in the CSNRZ modulated signal which is easily degraded by turbulence. However, both DQPSK and PolSK encrypt data on signal phase and SOP which are highly robust to harsh and unforeseen air medium variations. Moreover, HG00 is the best-performing mode.

Table 4 Received signal eye diagram at 540 m range under light dust condition.

	HG00 Channel	HG01 Channel
CSNRZ	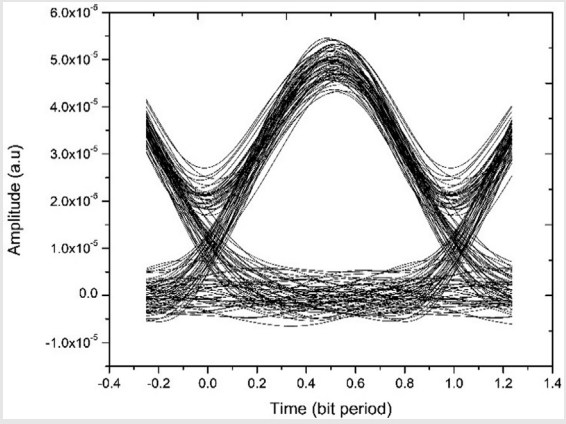	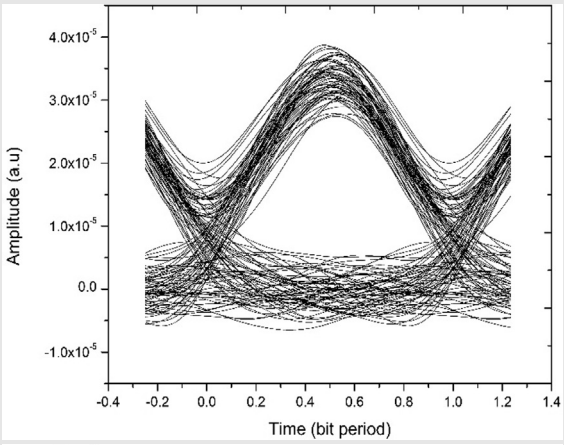
DQPSK (for in-phase signal)	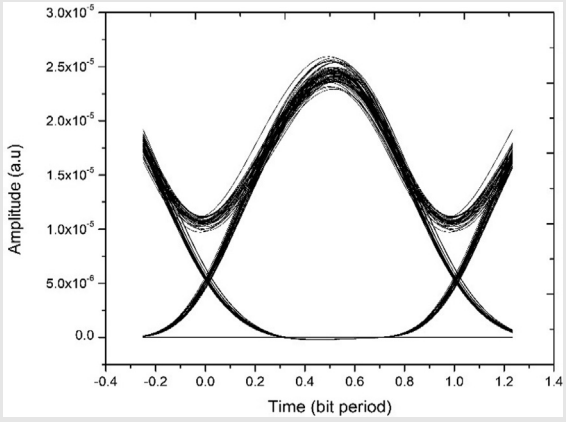	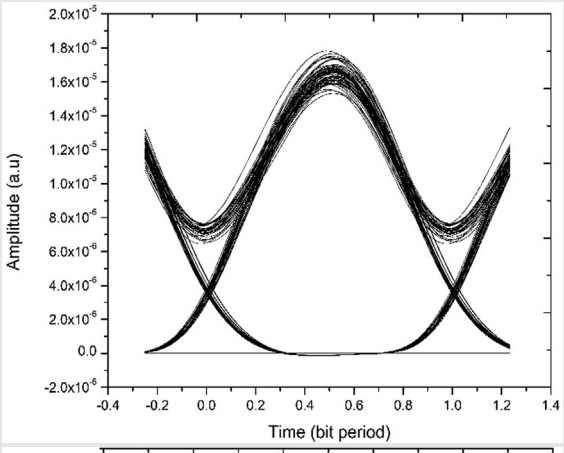
PolSK	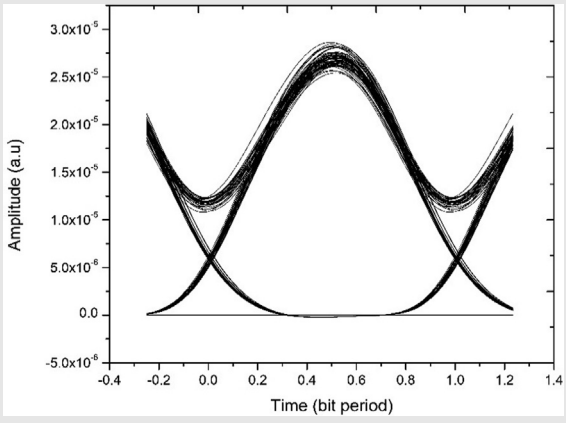	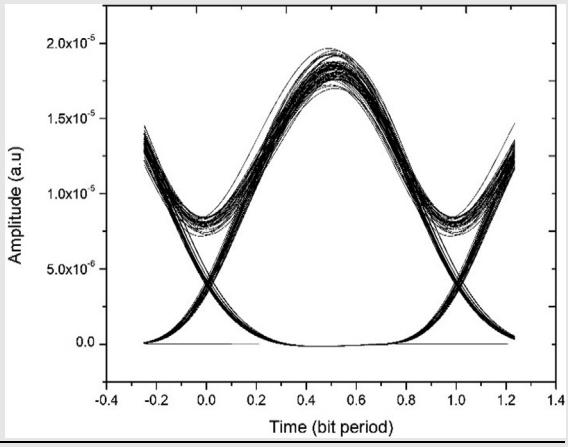

Tables 3-6 report eye diagrams of the received 3D modulated signal (CSNRZ-DQPSK-PolSK) at maximum acquired distances for the four different dust conditions. Different link range are considered for different weather conditions while computing eye diagrams, since visibility for each weather is different. The wide eye-opening and high eye height with satisfactory Q-factor values establish successful retrieval of the 120 Gbps data signal at the optical detector.

Table 5 Received signal eye diagram at 170 m range under medium dust condition.

	HG00 Channel	HG01 Channel
CSNRZ	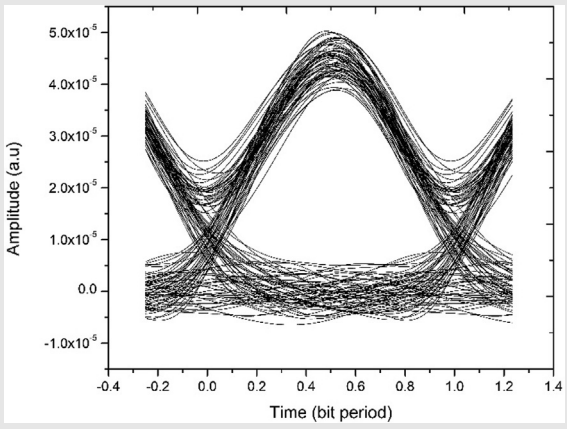	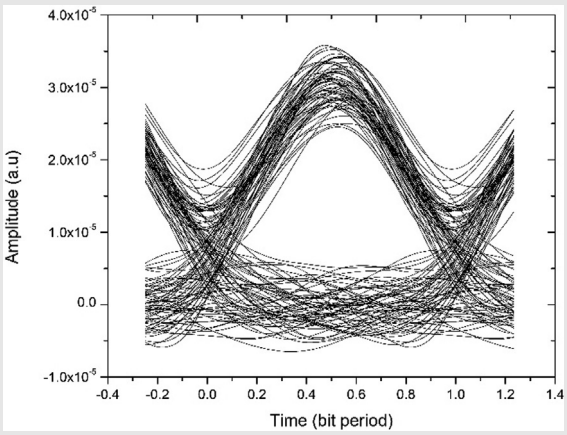
DQPSK (for in-phase signal)	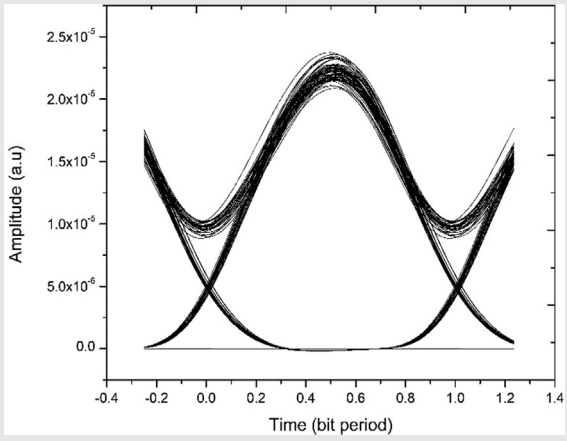	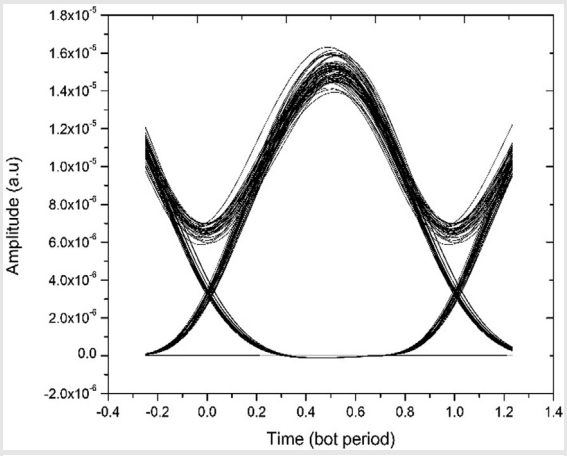
PolSK	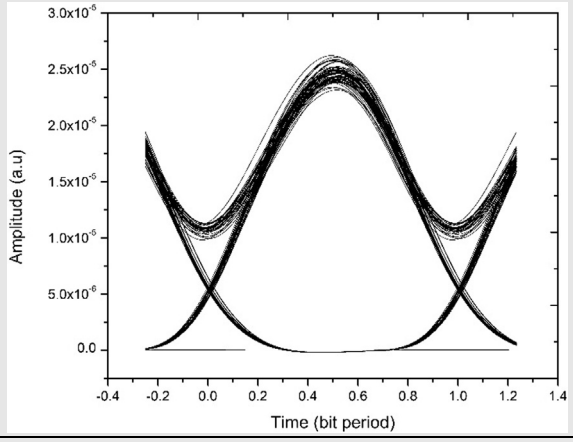	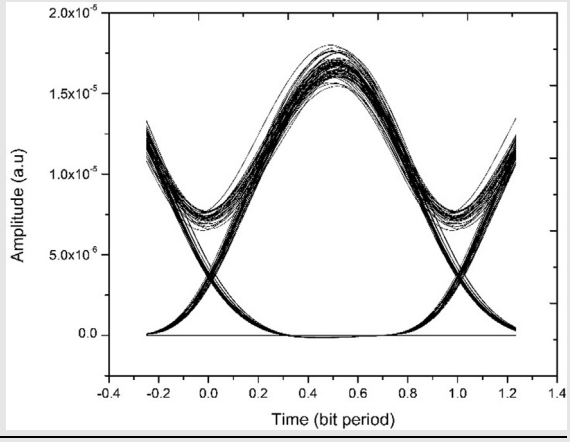

3.3. 3D modulated MDM-FSO system in foggy weather

Figs. 8-10 signify the Q-factor performance of the proposed system under low, moderate, and heavy fog conditions respectively. Both DQPSK and PolSK outperform the CSNRZ modulation scheme in fog situations also.

Tables 7-9 display the eye diagrams of a modulated signal comprising of CSNRZ, DQPSK, and PolSK at the maximum reach for the light, moderate, and heavy fog. Different link range are considered for different weather conditions while computing eye diagrams, since visibility for each weather is different. The clear and distinct eye pattern with reliable Q-factor values confirm the faithful reception of the 120 Gbps data by the detector. Due to the increase in water vapor condensation, the upper limit of transmission range declines from a low fog to a heavy fog event.

Table 6 Received signal eye diagram at 67 m range under dense dust condition.

	HG00 Channel	HG01 Channel
CSNRZ	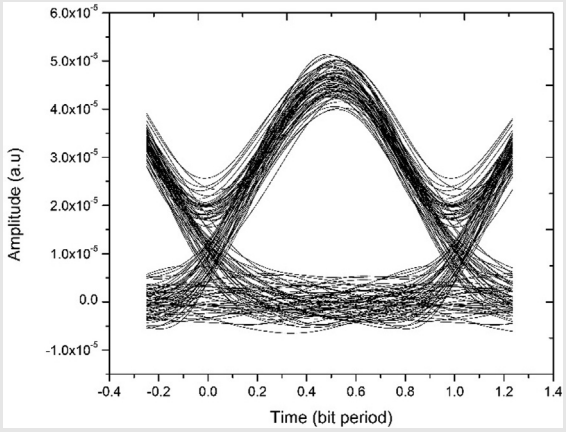	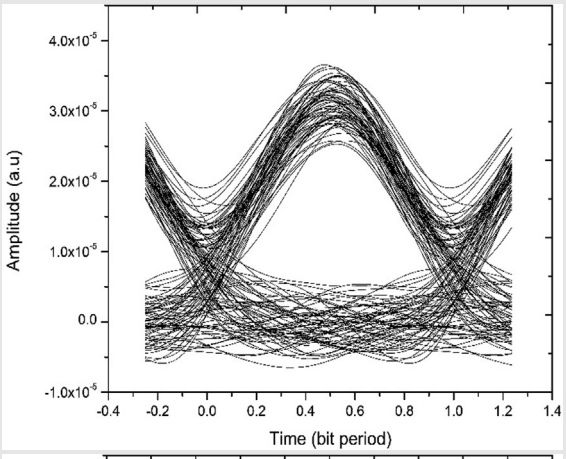
DQPSK (for in-phase signal)	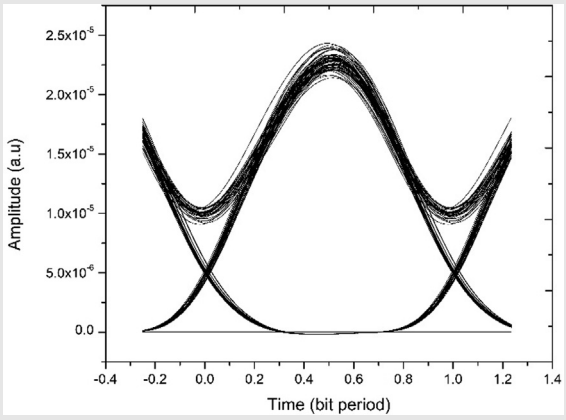	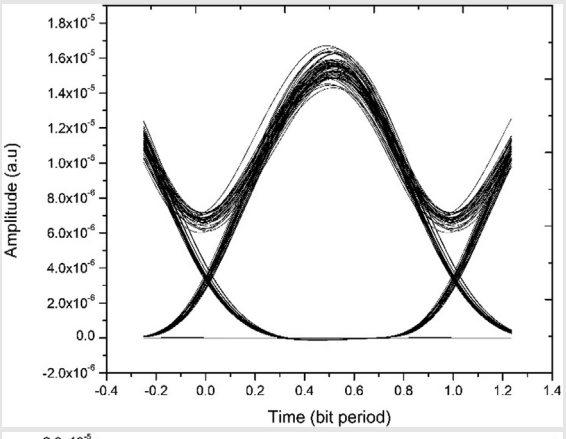
PolSK	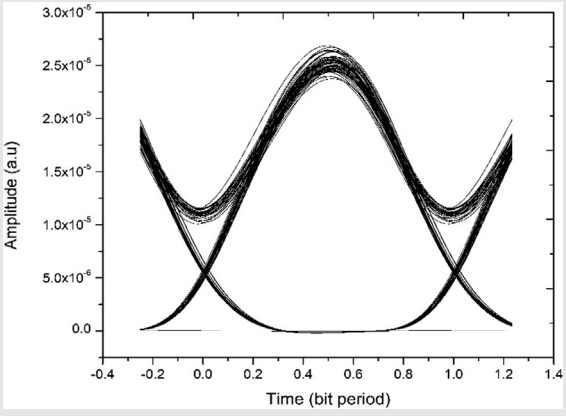	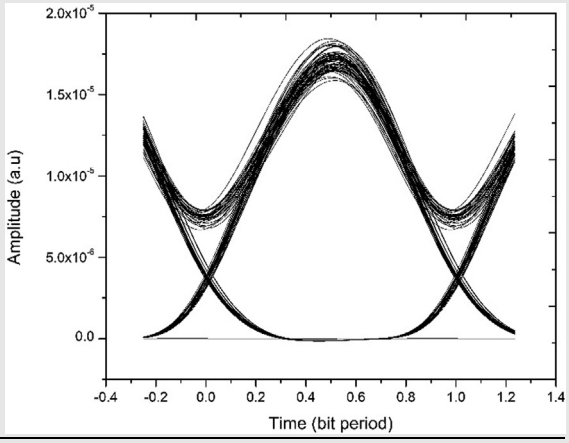

3.4. Comparison of dust and fog effects

Although the particle size in both fog and dust are alike, their compositions and effects on laser beams are different. Moreover, the dimension of particles in both fog and dust lies adjacent to the FSO signal wavelength. Conversely, the high water content in fog elements results in little scattering of the arriving signal. Table 10 shows that the FSO signal undergoes higher attenuation in the dusty air channel. The proposed system works at only a 67 m range in dense dust while a 200 m range

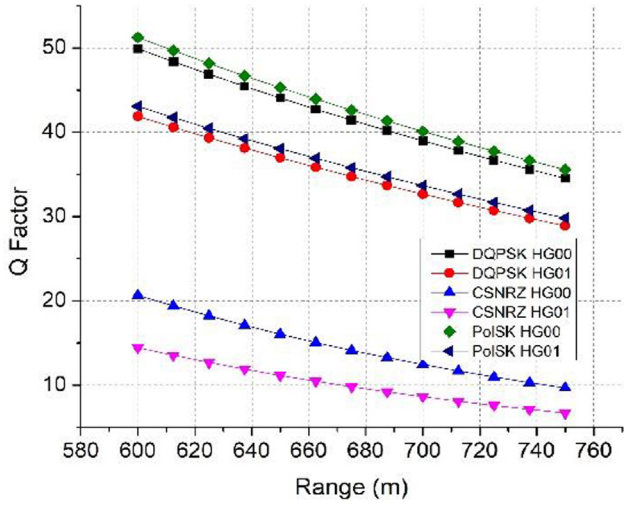

Fig. 8 Q-factor v/s range under low fog condition.

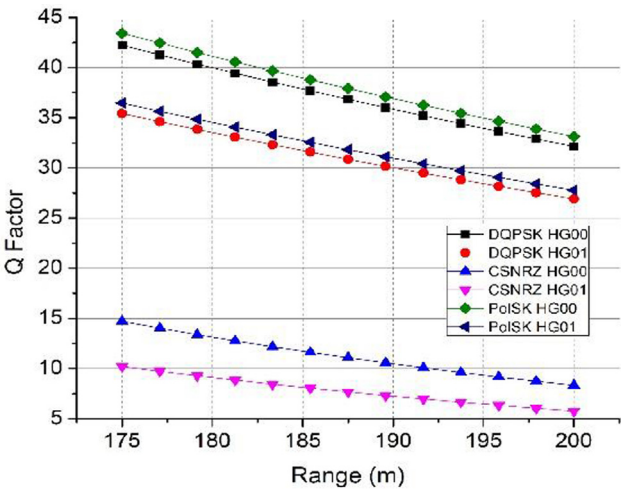

Fig. 10 Q-factor v/s range under heavy fog condition.

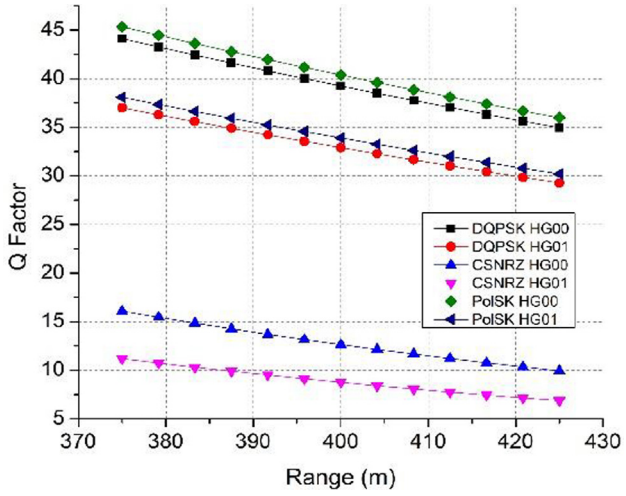

Fig. 9 Q-factor v/s range under moderate fog condition.

is achieved under heavy fog at less than 1/3rd of attenuation caused due to dust. Therefore, the implications of the dust storm on FSO are more terrible than fog.

3.5. Case studies for the deployment of the proposed system in disaster-hit regions

A layer of dense to very dense fog was witnessed over the Delhi Noida Direct flyway and surrounding parts of the Delhi-NCR region on February 13, 2021, with an air quality index (AQI) of 307 (nominal AQI is 0–50). This decreased the visibility range beyond the minimum threshold. Violent dust currents struck North India in 2018 in a chain of three dust events (DE1, DE2, DE3) on 2/3, 7/8, and 12/13 May. These dust storms affected the air quality of all key cities and villages. As per the Indian Meteorological Department report, the wind speed hit a record of 100 km/hr in the course of DE1, DE2, and DE3. More than 155 people were killed and many were injured. These strong winds left many base transceiver stations damaged and fiber cables broken. The major issue during the dust storm and after that was the cellular and data communication blackout. In these situations, the proposed FSO communication system can be established to provide a fast high-capacity internet connection to facilitate search and rescue team and establish data services within the area until the RF infrastructure is restored.

4. Conclusion

We present the concept and implementation of 3D hybrid optical modulation based on concurrent modulation of CSNRZ, DQPSK, and PolSK schemes for MDM-FSO-enabled B5G applications with efficient utilization of bandwidth and channel capacity. The outcomes indicate that the new modulation format provides substantial benefits with amplified spectral efficiency at acceptable Q factor values all through the maximum reach in challenging environments. The proposed system accomplishes successful 120 Gbps data transmission through 4 km FSO range in clear weather; 1250 m, 540 m, 170 m, and 67 m under very light, light, moderate, and dense dust; and 750 m, 425 m, and 200 m in light, moderate, and heavy fog, respectively with an acceptable Q Factor (i.e. ≥ 6). The system is analyzed for disaster management activities and thus real-time case studies have been considered for the practical implementation of the proposed MDM-FSO system in high attenuation and extreme environments.

Funding acknowledgement

Project of Excellence No. 2214/2022-2023, Faculty of Science, University of Hradec Králové.

Declaration of Competing Interest

The authors declare that they have no known competing financial interests or personal relationships that could have appeared to influence the work reported in this paper.

Table 7 Received signal eye diagram at 750 m range under low fog condition.

	HG00 Channel	HG01 Channel
CSNRZ	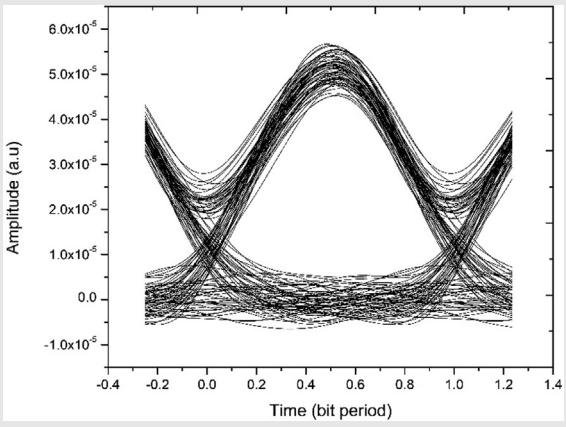	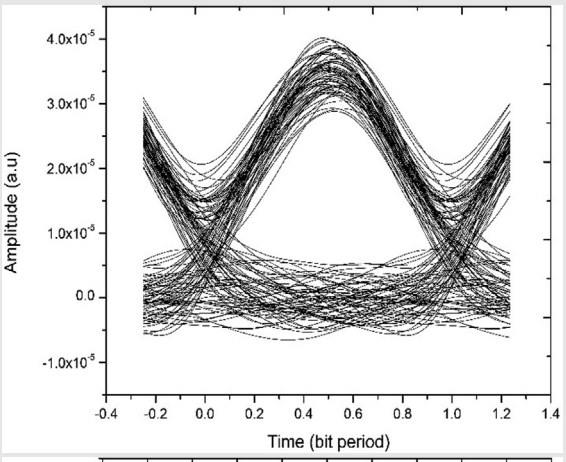
DQPSK (for in-phase signal)	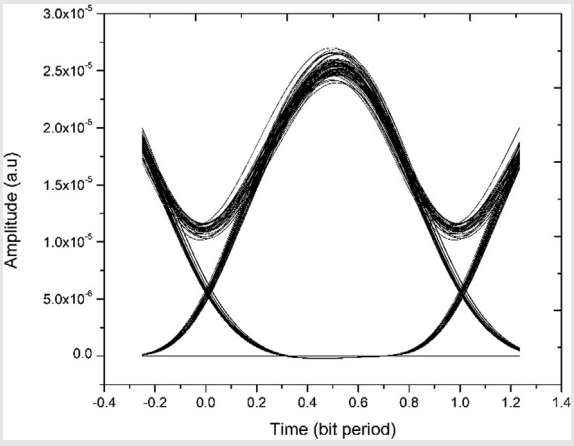	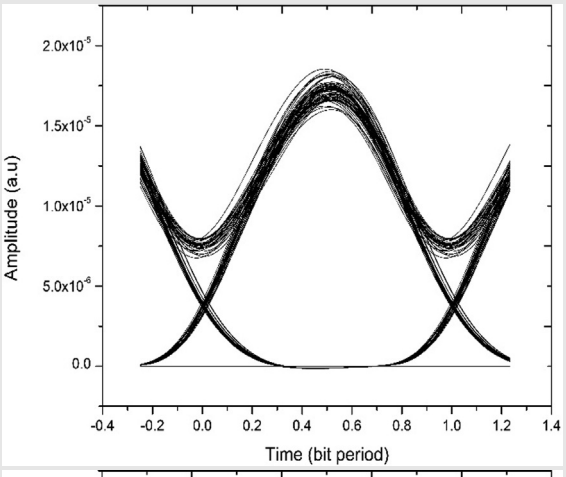
PolSK	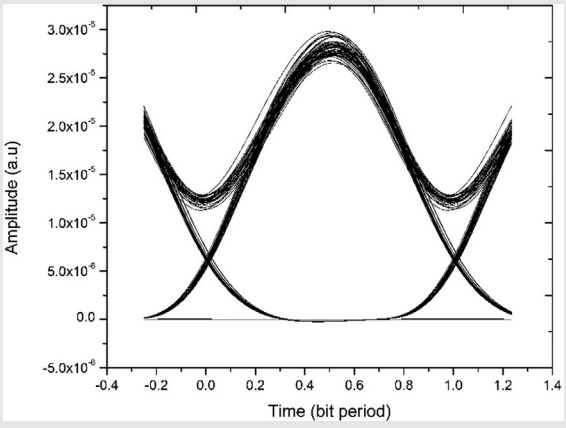	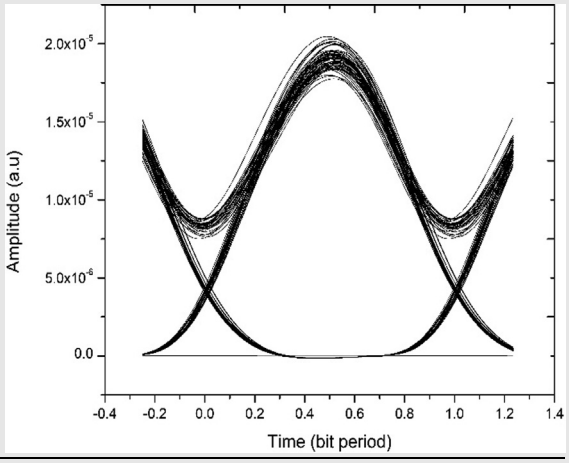

Table 8 Received signal eye diagram at 425 m range under medium fog condition.

	HG00 Channel	HG01 Channel
CSNRZ	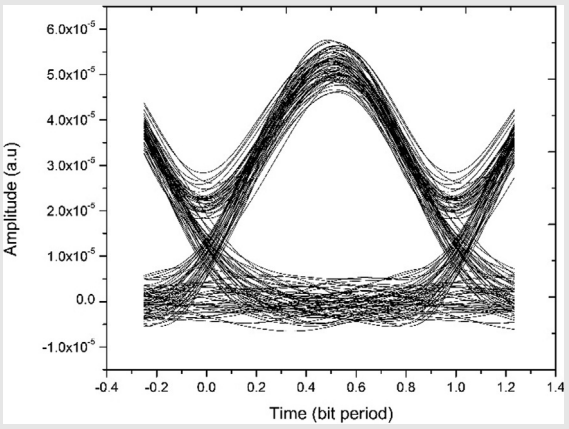	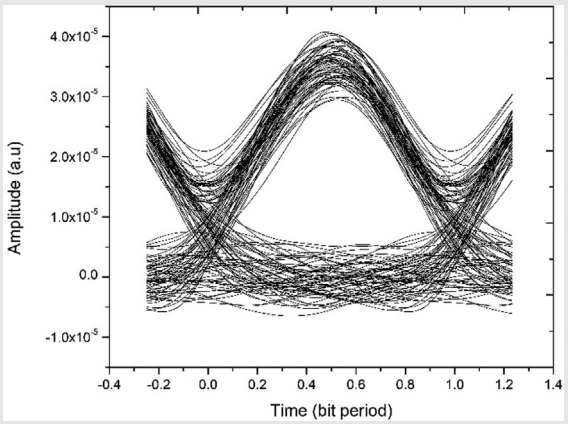
DQPSK (for in-phase signal)	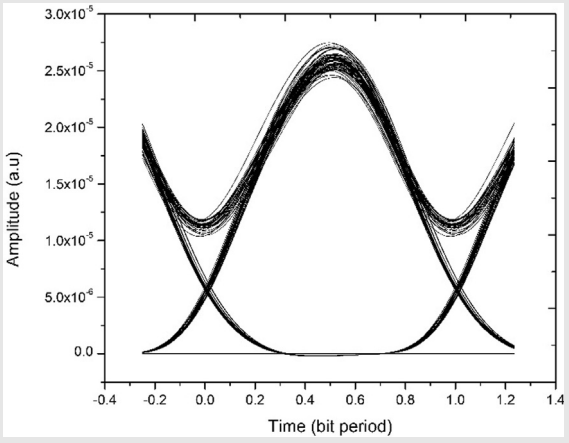	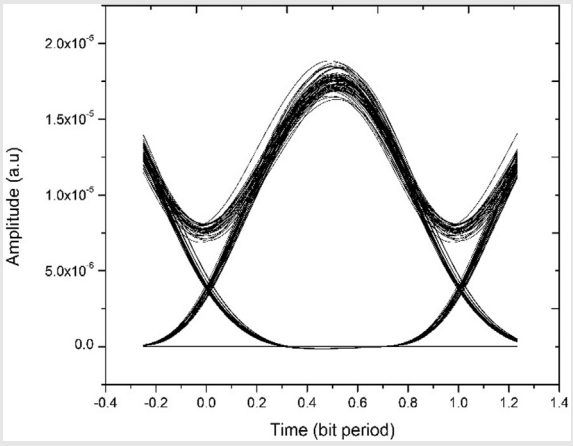
PolSK	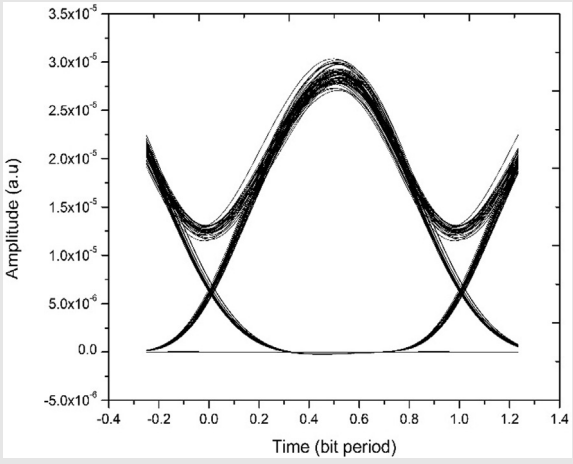	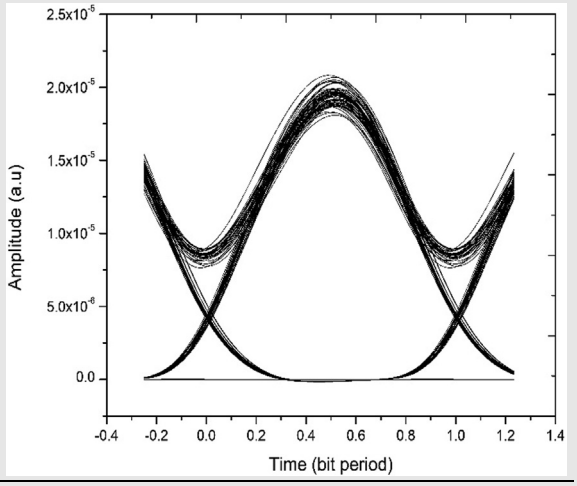

Table 9 Received signal eye diagram at 200 m range under heavy fog condition.

	HG00 Channel	HG01 Channel
CSNRZ	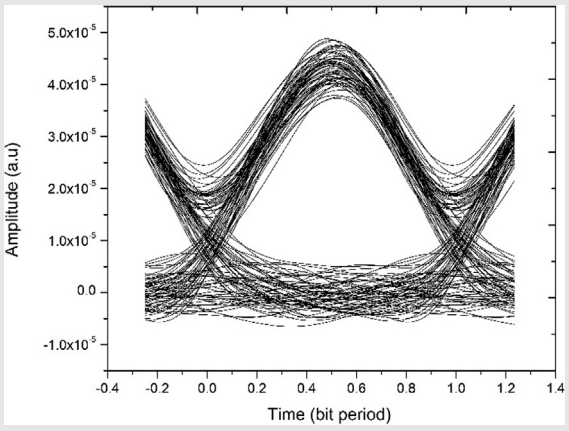	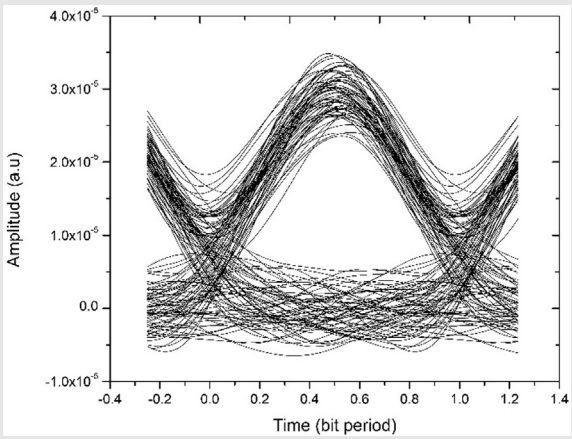
DQPSK (for in-phase signal)	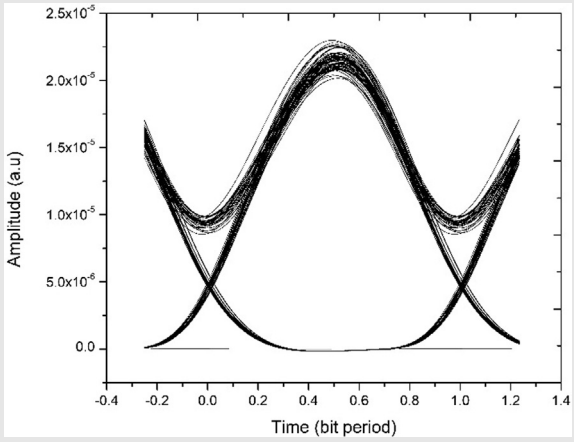	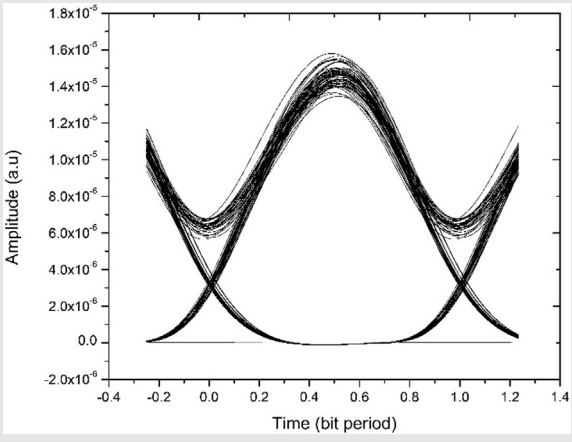
PolSK	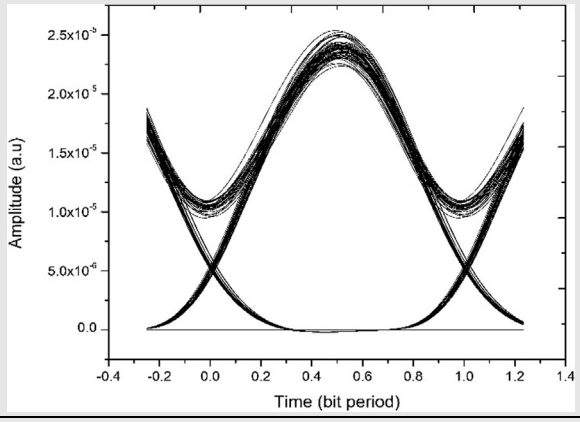	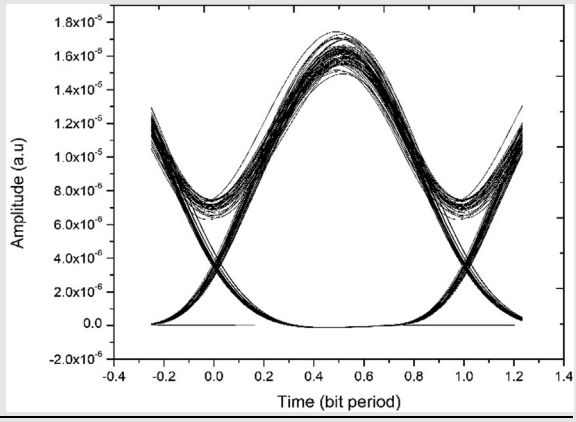

Table 10 Performance comparison of the proposed system in dust and fog.

Type of weather under analysis		Range (m)	Attenuation (dB/km)	Q-factor
Dust	Very Light	1250	6.73	35.99
	Light	540	25.11	35.03
	Moderate	170	107.66	33.62
	Dense	67	297.38	34.00
Fog	Low	750	15.55	35.57
	Medium	425	33.96	35.99
	Heavy	200	90	33.12

References

[1] M. Singh, J. Malhotra, A. Atieh, H.J. El-Khozondar, V. Dhasarathan, Performance investigation of 1.6 Tbps hybrid WDM-PDM-OFDM-based free space optics transmission link, Wireless Personal Commun. 117 (3) (2021) 2285–2309, https://doi.org/10.1007/s11277-020-07972-1.

[2] S. Iqbal, A. Raza, M.F.U. Butt, J. Mirza, M. Iqbal, S. Ghafoor, M. El-Hajjar, Millimeter-wave enabled PAM-4 data transmission over hybrid FSO-MMPOF link for access networks, Opt. Rev. 28 (3) (2021) 278–288, https://doi.org/10.1007/s10043-021-00659-3.

[3] A.R. Palanisamy, G.M. Tamilselvan, A. Pushparaghavan, Design of high-speed 10-Gb/s wired/FSO systems for local area communication networks for maximum reach, Photonic Netw. Commun. 38 (2) (2019) 206–218, https://doi.org/10.1007/s11107-019-00860-0.

[4] S.N. Pottoo, R. Goyal, A. Gupta, Development of 32-GBaud DP-QPSK free space optical transceiver using homodyne detection and advanced digital signal processing for future optical networks, Opt. Quant. Electron. 52 (11) (2020), https://doi.org/10.1007/s11082-020-02623-y.

[5] J. Jeyaseelan, D. Sriram Kumar, B.E. Caroline, Disaster management using free space optical communication system, Photonic Netw. Commun. 39 (1) (2020) 1–14, https://doi.org/10.1007/s11107-019-00865-9.

[6] S.N. Pottoo, R. Goyal, A. Gupta, Performance investigation of optical communication system using FSO and OWC channel, Indo - Taiwan 2nd Int. Conf. Comput. Anal. Networks, Indo-Taiwan ICAN 2020 - Proc., pp. 176–180, 2020, doi: 10.1109/Indo-TaiwanICAN48429.2020.9181322.

[7] M. Singh, J. Malhotra, A high-speed long-haul wavelength division multiplexing-based inter-satellite optical wireless communication link using spectral-efficient 2-D orthogonal modulation scheme, Int. J. Commun Syst 33 (6) (2020) e4293, https://doi.org/10.1002/dac.v33.610.1002/dac.4293.

[8] S. Singh, S. Singh, R. Kaur, R.S. Kaler, Performance investigation of optical multicast overlay system using orthogonal modulation format, Opt. Commun. 338 (2015) 58–63, https://doi.org/10.1016/j.optcom.2014.10.033.

[9] M. Ohm, J. Speidel, Quaternary optical ASK-DPSK and receivers with direct detection, IEEE Photonics Technol. Lett. 15 (1) (2003) 159–161, https://doi.org/10.1109/LPT.2002.805776.

[10] Y. Shao, N. Chi, High spectral-efficiency 100Gbit/s transmission using DRZ, DQPSK, and PoISK three dimension orthogonal modulation, Opt. Commun. 285 (6) (2012) 1049–1052, https://doi.org/10.1016/j.optcom.2011.11.076.

[11] M. Singh, J. Malhotra, Performance investigation of high-speed FSO transmission system under the influence of different atmospheric conditions incorporating 3-D orthogonal modulation scheme, Opt. Quant. Electron. 51 (9) (2019), https://doi.org/10.1007/s11082-019-1998-2.

[12] S. Singh, R.S. Kaler, Performance investigation of Raman erbium-doped fiber amplifier hybrid optical amplifier in the scenario of high-speed orthogonal-modulated signals, Opt. Eng. 53 (3) (2014) 036102.

[13] A. Amphawan, S. Chaudhary, V. Chan, Optical millimeter wave mode division multiplexing of LG and HG modes for OFDM Ro-FSO system, Opt. Commun., 431 (January 2018), pp. 245–254, 2019, doi: 10.1016/j.optcom.2018.07.054.

[14] M. Singh, J. Malhotra, M.S. Mani Rajan, D. Vigneswaran, M. H. Aly, A long-haul 100 Gbps hybrid PDM/CO-OFDM FSO transmission system: Impact of climate conditions and atmospheric turbulence, Alexandria Eng. J. 60 (1) (2021) 785–794, https://doi.org/10.1016/j.aej.2020.10.008.

[15] M. Singh, S.N. Pottoo, J. Malhotra, A. Grover, M.H. Aly, Millimeter-wave hybrid OFDM-MDM radio over free space optical transceiver for 5G services in desert environment, Alexandria Eng. J. 60 (5) (2021) 4275–4285, https://doi.org/10.1016/j.aej.2021.03.029.

[16] M. Singh, J. Malhotra, A. Atieh, D. Kakati, D. Vigneswaran, Investigation of 340-Gbps terrestrial FSO link incorporating spectral-efficient DP-QPSK-PolSK hybrid modulation scheme, Opt. Eng., 59(11), Article ID-116106, doi: 10.1117/1.OE.59.11.116106.

[17] M. Alibakhshikenari, B.S. Virdee, L. Azpilicueta, M. Naser-Moghadasi, M.O. Akinsolu, C.H. See, B.o. Liu, R.A. Abd-Alhameed, F. Falcone, I. Huynen, T.A. Denidni, E. Limiti, A Comprehensive Survey of "Metamaterial Transmission-Line Based Antennas: Design, Challenges, and Applications", IEEE Access 8 (2020) 144778–144808, https://doi.org/10.1109/ACCESS.2020.3013698.

[18] M. Alibakhshikenari, E.M. Ali, M. Soruri, M. Dalarsson, M. Naser-Moghadasi, B.S. Virdee, C. Stefanovic, A. Pietrenko-Dabrowska, S. Koziel, S. Szczepanski, E. Limiti, A Comprehensive Survey on Antennas On-Chip Based on Metamaterial, Metasurface, and Substrate Integrated Waveguide Principles for Millimeter-Waves and Terahertz Integrated Circuits and Systems, IEEE Access 10 (2022) 3668–3692, https://doi.org/10.1109/ACCESS.2021.3140156.

[19] M. Alibakhshikenari, F. Babaeian, B.S. Virdee, S. Aissa, L. Azpilicueta, C.H. See, A.A. Althuwayb, I. Huynen, R.A. Abd-Alhameed, F. Falcone, E. Limiti, A Comprehensive Survey on "Various Decoupling Mechanisms With Focus on Metamaterial and Metasurface Principles Applicable to SAR and MIMO Antenna Systems", IEEE Access 8 (2020) 192965–193004, https://doi.org/10.1109/ACCESS.2020.3032826.

[20] M. Alibakhshikenari, B.S. Virdee, C.H. See, R.A. Abd-Alhameed, F. Falcone, E. Limiti, Automated Reconfigurable Antenna Impedance for Optimum Power Transfer, IEEE Asia-Pacific Microwave Conference (APMC) 2019 (2019) 1461–1463, https://doi.org/10.1109/APMC46564.2019.9038260.

[21] M. Alibakhshikenari, B.S. Virdee, P. Shukla, Y. Wang, L. Azpilicueta, M. Naser-Moghadasi, C.H. See, I. Elfergani, C.

Zebiri, R.A. Abd-Alhameed, I. Huynen, J. Rodriguez, T.A. Denidni, F. Falcone, E. Limiti, Impedance Bandwidth Improvement of a Planar Antenna Based on Metamaterial-Inspired T-Matching Network, IEEE Access 9 (2021) 67916–67927, https://doi.org/10.1109/ACCESS.2021.3076975.

[22] M. Alibakhshikenari, B.S. Virdee, C.H. See, R.A. Abd-Alhameed, F. Falcone, E. Limiti, Impedance Matching Network Based on Metasurfaces (2-D Metamaterials) for Electrically Small Antennas, IEEE International Symposium on Antennas and Propagation and North American Radio Science Meeting 2020 (2020) 1953–1954, https://doi.org/10.1109/IEEECONF35879.2020.9330460.

[23] M. Alibakhshikenari, B.S. Virdee, C.H. See, R.A. Abd-Alhameed, F. Falcone, E. Limiti, Metasurface for Controlling Polarization of Scattered EM Waves, in: 2020 4th Australian Microwave Symposium (AMS), 2020, pp. 1–2, https://doi.org/10.1109/AMS48904.2020.9059504.

[24] I. Nadeem, M. Alibakhshikenari, F. Babaeian, A.A. Althuwayb, B.S. Virdee, L. Azpilicueta, S. Khan, I. Huynen, F. Falcone, T. A. Denidni, E. Limiti, A comprehensive survey on 'circular polarized antennas' for existing and emerging wireless communication technologies, J. Phys. D Appl. Phys. 55 (3) (2022) 033002, https://doi.org/10.1088/1361-6463/ac2c36.

[25] M. Alibakhshikenari, B.S. Virdee, C.H. See, R.A. Abd-Alhameed, F. Falcone, E. Limiti, Energy Harvesting Circuit with High RF-to-DC Conversion Efficiency, 2020 IEEE International Symposium on Antennas and Propagation and North American Radio Science Meeting (2020) 1299–1300, https://doi.org/10.1109/IEEECONF35879.2020.9329604.

[26] M. Alibakhshikenari, B.S. Virdee, P. Shukla, C.H. See, R.A. Abd-Alhameed, F. Falcone, E. Limiti, Improved adaptive impedance matching for RF front-end systems of wireless transceivers, Sci. Rep. 10 (1) (2020), https://doi.org/10.1038/s41598-020-71056-0.